Research Square

Preprints are preliminary reports that have not undergone peer review.
They should not be considered conclusive, used to inform clinical practice,
or referenced by the media as validated information.

3D Multiscan Stitching enables Large-Volume-Recording of Abdominal Ultrasound Imaging in Phantoms and Patients

Valentin Blank

valentin.blank@uk-halle.de

Halle University Medical Center

Paula Schwabe

Evangelisches Diakonissenkrankenhaus Leipzig

Johannes Wiegand

Leipzig University Medical Center

Thomas Karlas

Leipzig University Medical Center

Research Article

Keywords: tomographic ultrasound, multi-scan, large-area ultrasound, volume stitching, three-dimensional (3D) imaging

Posted Date: July 7th, 2026

DOI: https://doi.org/10.21203/rs.3.rs-9836142/v1

License: This work is licensed under a Creative Commons Attribution 4.0 International License. Read Full License

Additional Declarations: Competing interest reported. This work was supported by the Federal Ministry of Education and Research (BMBF) through a MetaRot Grant from the Integrated Research and Treatment Center AdiposityDiseases Leipzig (IFB), Germany, FKZ01EO1001. The funders had no role in the study design, data collection and analysis, decision to publish, or preparation of the manuscript.

Abstract

Background

Conventional ultrasound is widely used in abdominal imaging but remains limited by operator dependency, non-standardized documentation, and a restricted field of view. Tomographic three-dimensional ultrasound combined with multiscan stitching may overcome some of these limitations by generating standardized large-volume datasets that allow retrospective multiplanar review. This pilot study evaluated the technical feasibility of multiscan three-dimensional ultrasound for large-volume abdominal imaging in phantoms, healthy volunteers, and selected patients with liver disease.

Methods

A multiscan stitching algorithm was first assessed under controlled conditions using standardized ultrasound phantoms to evaluate volume reconstruction, seam continuity, and artifact formation. The method was then prospectively applied in 22 healthy volunteers and 22 patients with focal or chronic parenchymal liver disease. Conventional ultrasound served as the reference for image quality and completeness of organ depiction. Additional phantom and proof-of-concept torso examinations were performed to explore potential future use cases.

Results

In phantom experiments, adjacent three-dimensional ultrasound volumes could be successfully merged, with preserved margin continuity when acquisition was performed under standardized conditions and with sufficient overlap. In healthy volunteers, three-dimensional ultrasound enabled large-area abdominal and liver coverage, although image quality was lower than conventional B-mode ultrasound and varied depending on the scan protocol. In patients, focal liver lesions and characteristic features of diffuse liver disease were visualized in reconstructed datasets. The best balance between image quality and organ coverage was achieved with acquisition strategies using fewer, well-aligned adjacent volumes. Stitching-related artifacts, respiratory motion, transducer pressure, and tracking-related limitations were identified as relevant technical challenges.

Conclusion

Multiscan tomographic three-dimensional ultrasound is technically feasible for generating standardized large-volume abdominal ultrasound datasets in phantoms, healthy volunteers, and selected patients under favourable examination conditions. The approach may support retrospective examiner-independent review, structured documentation, telemedical assessment, and future image-analysis workflows. However, the findings remain exploratory and system-specific. Quantitative validation of geometric accuracy, diagnostic performance, reproducibility, and robustness in larger and more heterogeneous patient cohorts is required before broader clinical implementation.

Trial registration

The study was registered in the German Clinical Trials Register (DRKS00016736 05/2019).

Background

Ultrasound is an excellent diagnostic modality that is indispensable in numerous medical specialties, particularly for point-of-care imaging. Its applications range from highly focused emergency sonography [1] to the differential diagnostic

evaluation of focal liver lesions [2]. In visceral medicine, ultrasound is often considered the first-line imaging method for many indications, due to its broad availability and lack of ionizing radiation [3].

However, the diagnostic value of ultrasound depends substantially on the examiner's expertise and training [4,5]. The documentation typically consists of non-standardized two-dimensional images, adding difficulty to the subsequent interpretation by other physicians. This operator-dependent nature contrasts with cross-sectional imaging modalities, which rely on standardized protocols and routinely store dedicated scanning procedures in defined anatomic planes [6].

Overcoming these limitations and establishing standardized workflows that enable retrospective image analysis are paramount for future ultrasound applications in many fields, e.g., for staging and following patients with cancer, sharing data across institutions, and employing advanced post-processing or automated analyses with emerging artificial intelligence tools [7].

Modern echocardiography illustrates the potential for such standardization. Specialized 4D matrix probes have already been established in routine care for acquiring standardized echocardiographic datasets, which can subsequently be evaluated and measured in a consistent manner [8]. Similarly, 3D probes in gynaecology offer analogous approaches [9].

Several comprehensive reviews have established the technical foundations and clinical potential of three-dimensional ultrasound imaging and have highlighted its emerging value for abdominal applications, while emphasizing persisting limitations related to acquisition, registration, and fusion of large anatomical volumes [10–12]. This is especially relevant for abdominal ultrasound examinations capture substantially larger and more spatially complex organ systems compared with the relatively confined anatomy encountered in cardiac imaging. Although promising results exist for capturing extended 3D sweeps in the abdomen [13], a limited transducer width prevents the capture of the entire abdomen or complete organ systems. Specialized software solutions are therefore required to merge multiple scans into one large-volume dataset [14].

These "stitching" algorithms aim to seamlessly integrate multiple adjacent 3D ultrasound acquisitions into a single, comprehensive volume, akin to the panoramic image mode on a smartphone—but in three dimensions [15]. While stitching techniques have been applied to smaller, superficial organs using linear transducers [16], they have not been systematically evaluated for large-scale abdominal diagnostics. In the field of ultrasound education, similar techniques are already being used to simulate larger abdominal organs in modern ultrasound simulators [17].

As previously mentioned, research has shown that combining tracked and tracker-less 3D ultrasound across cardiac, foetal, and breast applications maintains geometric fidelity and enhances image quality [18–21]. Our work extends these concepts to the technically more challenging deep-abdominal setting with convex probes and respiratory motion.

Therefore, in this study, we evaluated a novel ultrasound system designed to generate a metrically accurate abdominal volume via multiple standardized 3D ultrasound acquisitions. This study is preliminary and intended as a feasibility assessment. To our knowledge, this is the first comprehensive evaluation of stitching-based technology for abdominal diagnostics using ultrasound in a diagnostic approach.

Methods

Study design

This pilot study aimed to evaluate the applicability and technical feasibility of a novel multiscan stitching algorithm for abdominal 3D ultrasound (3DUS) volumes acquired with a conventional curved-array transducer.

First, technical performance was assessed under controlled in vitro conditions using a standardized ultrasound phantom to verify volumetric reconstruction and stitching behaviour.

Second, the approach was transferred to the in vivo setting to evaluate the feasibility of large-area liver coverage and organ depiction in healthy volunteers, and to assess the delineation of focal and diffuse liver pathology in a selected clinical cohort evaluation image quality and organ depiction.

Finally, potential clinical use scenarios (e.g., standardized training/education and pre-clinical evaluation of acquisition strategies) were demonstrated using a neonatal torso phantom and an adult human torso (see **Figure 1**).

Ethics approval and consent to participate

The study was performed in accordance with the guidelines for good clinical practice (ICH-GCP E6/R1) and the ethical guidelines of the Helsinki Declaration. The local ethics committee of the University of Leipzig approved the study (approval/registration number 059/19-ek), and it was registered in the German Clinical Trials Register (DRKS00016736). All participants provided written informed consent, and all ultrasound methods were approved for medical use.

Technical evaluation of the stitching algorithm using ultrasound phantoms

The technical applicability and quality of the stitched volumes were evaluated via a standardized ultrasound phantom based on a gelatine matrix supplemented with water-filled ballons and inclusions that create well-defined boundaries for assessing seam continuity and margin depiction (see **Figure 1A**). Further details on the phantom are described in Seitzinger et al. 2024 [40]. Four adjacent ultrasound volumes with different overlapping areas were stored using 3DUS. We systematically varied the nominal overlap between adjacent acquisitions by adjusting sweep start/stop landmarks to achieve approximately 1–3 cm of physical overlap.

In addition, we used a commercially available ultrasound phantom of a paediatric torso made of polyurethane elastomer with an approximate size of 41 × 17 × 15 (Paediatric FAST/Acute Abdomen Phantom" (Kyoto Kagaku)) [41,42] to provide proof-of-concept data for future clinical applications (see **Figure 1C**).

Study population

The 3DUS method was prospectively evaluated in a cohort of healthy volunteers, all of whom exhibited a body mass index (BMI) < 25 kg/m^2 and no detectable pathologies in the examination area, to ensure optimal examination conditions (**see Figure 1B**).

In an exploratory approach, suitable patients with previously diagnosed focal or chronic parenchymal liver diseases were recruited for 3DUS assessment under routine clinical conditions. These patients were scheduled for standard ultrasound evaluations due to common pathologies, including hemangioma or focal nodular hyperplasia (FNH) larger than 1 cm in the liver, metabolic-associated steatotic liver disease (MASLD), or liver cirrhosis (**see Table 1 and Figure 1B**). The exclusion criteria included technical (pacemaker, due to potential interference with the magnetic field) and ethical (age <18 years and >80 years, pregnancy, malignant pathology) reasons as well as image quality factors (BMI > 30 kg/m^2, impaired imaging due to meteorism or postsurgery).

Conventional ultrasound (conUS) examination

Conventional ultrasound served as the reference standard for both image quality and examination completeness. All participants underwent a standardized ultrasound evaluation of the liver and surrounding abdominal organs via a high-end ultrasound system (Aplio i800, Canon Medical Systems, Japan) equipped with a multifrequency curved-array high-performance matrix transducer (i8CX1). An experienced examiner (PS) performed the ultrasound after a fasting period of at least four hours. Patient positioning and breathing were optimized (for example, placing the patient on the left side) to minimize interference from intestinal air. The examination was documented through a comprehensive video loop and standardized image planes, sweeping from the left liver lobe to the right liver lobe in the sagittal plane. All acquisitions were

performed using optimized, standardized imaging presets, with real-time adjustments (e.g., gain and related parameters) tailored to ensure optimal image quality.

Tomographic three-dimensional ultrasound (3DUS) using a multiscan stitching algorithm

Immediately after the conventional ultrasound (conUS) examination, 3DUS images were recorded using a stand-alone 3D ultrasound system (PIUR Imaging, Software V1.1, Vienna, Austria). For 3D ultrasound acquisition, we used the same scanner settings as for the conventional ultrasound examination. The applied 3D ultrasound device is a commercially available CE-marked diagnostic device approved for medical use. Briefly, astand-alone workstation captured the live 2D B-mode video output from the ultrasound system via an HDMI/DVI frame-grabber and synchronized it with probe pose data. For spatial tracking, the conventional ultrasound probe was equipped with an electromagnetic sensor **(Figure 2A)** that recorded probe position and orientation within a low-frequency magnetic field generated by an external field generator[43–45].

Technical background: magnetically tracked ultrasound acquisition combines real-time transducer pose recording with conventional B-mode imaging to spatially register each 2D frame within a common three-dimensional coordinate system[45]. After sensor-to-image calibration and time synchronization, each frame can be mapped into patient space to reconstruct a metric 3D ultrasound volume. In this context, “metric” refers to voxels defined in a patient-fixed coordinate system calibrated in millimetres based on the tracking system and the ultrasound scanner’s imaging geometry, enabling distance and volume measurements. The absolute voxel size depends on the native resolution of the ultrasound video output and the size of the examined field of view. The PIUR software reconstructed the datasets on an automatically generated millimetre-calibrated 3D grid depending on the number of stitched sub-volumes and the anatomical field of view. No additional super-resolution reconstruction was applied; therefore, the effective spatial resolution remained limited by the native B-mode image quality, acoustic beam geometry, tracking accuracy, and interpolation during volume compounding. The electromagnetic tracking subsystem provides sub-millimeter positional accuracy (<1 mm) under ideal conditions, thereby supporting millimetre-calibrated measurements [46]. Franz et al. [47] provide a comprehensive overview of the physical principles, typical system architectures, and validation concepts for electromagnetic tracking in image-guided applications.

A key differentiator of the PIUR Imaging approach (PIUR Imaging Software V1.1) is that electromagnetic tracking is used not only to localize single acquisitions, but also to establish the relative spatial relationship between multiple consecutively acquired volumes (**Figure 3B and Supplementary Material 1**). This enables a physics-based pre-alignment of several volumetrically tracked datasets, while the subsequent overlay (“stitching”) refines alignment and continuity by algorithmic optimization (e.g., rigid and deformable registration, see below) [19].

In this way, the applied 3DUS software (PIUR Imaging Software V1.1) reconstructed the synchronized ultrasound video output and magnetic tracking data into three-dimensional ultrasound volumes of the scanned regions (**Figure 2B**). Adjacent volumes were acquired with a nominal physical overlap of approximately 2–3 cm at the target depth to support robust registration. Next, the adjacent 3D datasets were merged into a single comprehensive large-scale volume (**Figure 3**) using a stitching algorithm that integrates the recorded spatial tracking information and in addition evaluates overlapping border regions using a two-stage registration strategy. For this purpose, first, a rigid registration aligns volumes based on stable anatomical landmarks (e.g., large vessels or good visible boundaries), followed by a deformable refinement focused on the overlap regions to improve continuity and overall image quality. The deformable registration method then adapts the boundary regions of the individual volumes using a complex algorithm so that, for example, vascular courses and anatomical structures are optimally superimposed, thereby reducing potential artifacts caused by respiratory motion or varying transducer pressure. Comparable deformable registration concepts are also routinely applied in MRI image reconstruction and fusion workflows.

In this study, we evaluated different acquisition strategies and assessed a total of six distinct scanning scenarios (see Supplementary Material 1). These scenarios differed with respect to the relative orientation of the consecutively acquired

sub-volumes (e.g., sagittal versus transverse sweeps) and the number of individual acquisitions per dataset. Across all scenarios, the overarching goal was to enable a feasible, near-complete volumetric coverage of the entire liver.

Rating of the ultrasound image quality and completeness of organ visualization

The recorded ultrasound datasets were evaluated according to predefined anatomical and technical characteristics. A single examiner (PS) assessed all conventional ultrasound (conUS) examinations using a four-point ordinal scale (1 = insufficient to 4 = excellent) for each category. A second reviewer (VB), blinded to the conUS images and ratings, independently applied the same scale to the 3D datasets (**see Supplement 2 for details**).

Statistical analysis

Summary statistics for metric variables with symmetric distributions are presented as the means ± standard deviations (X ± Y). The quality criteria were evaluated via an ordinal scale. For method comparison, the mean 3DUS rating was expressed as a percentage of the mean conUS rating, which served as the reference standard. Diagnostic concordance was reported as a percentage indicating the proportion of cases in which 3DUS and conUS received identical scores, thus reflecting consistent clinical diagnostic criteria.

Results

Technical validation using an ultrasound phantom

The scanning and recording time for four adjacent longitudinal ultrasound scans (each covering 40 cm in length) was less than 60 seconds. Visualization of the embedded structures simulating focal lesions with well-defined margins demonstrated that the reconstructed 3D volumes preserved margin continuity and spatial coherence across adjacent acquisitions. Figure 3 illustrates the underlying acquisition and stitching workflow, including the use of partially overlapping volumes and subsequent postprocessing. In 3DUS, the outer boundaries of the embedded structures are accurately visualized, and no significant motion or overlay artifacts are observed with uniform, steady transducer guidance. However, if the transducer was poorly guided—for instance, tilted excessively or moved along a meandering path—noticeable motion artifacts occurred. Consistent with registration theory, increased physical overlap improved seam continuity and reduced local intensity mismatch within the overlap. An overlapping zone of approximately 2–3 cm was required to achieve optimal results.

Application of 3DUS in healthy volunteers

Twenty-two healthy volunteers were included in the study (see **Table 1**), and 3DUS was successfully performed in all the patients. The scanning times were similar for conUS and 3DUS (**Table 1**), though procedural times, including system setup for 3DUS, were longer due to retrospective analysis needs. Nevertheless, conUS includes ultrasound examination and simultaneous diagnostic interpretation, while 3DUS only respects the recording time of all six scans, and the diagnostic review occurred retrospectively. The reconstruction and stitching time depend on the number and size of the volumes recorded and usually takes less than a minute.

Across all the scans, 3DUS yielded consistently lower image quality scores than did conUS. The highest image quality (91%) for comprehensive liver visualization was achieved with a single sagittal sweep from the left to the right liver lobe (**Scan 6 – Supplement 1**), which did not require volume stitching. However, this method covered less of the entire liver (**Table 1 and Supplement 3**). The completeness of organ coverage varied among the different 3D scan protocols; for example, three parallel craniocaudal sweeps (**Scan 5 - Supplement 1**) provided the best imaging of the left kidney but inferior depiction of the left liver lobe.

An optimal balance between sufficiently high image quality (79%) and good completeness (73%) was achieved by merging two adjacent sagittal sweeps from the left and right lobes (**Scan 3, Supplement 1**). Notably, any stitching approach can result in image detail loss during the stitching process. Further details are provided in **Supplement 3**.

Implementation of 3DUS in suitable patients

Twenty-two patients with focal lesions or chronic parenchymal liver pathologies with an anticipated good examination quality were recruited for the study (**Table 1**). Tomographic 3D ultrasound (3DUS) was successfully performed in all patients, enabling visualization of all focal lesions and key characteristics of chronic liver disease on 3DUS. Overall, image quality and organ completeness were comparable or even superior to findings in healthy volunteers via 3DUS. Diagnostic assessments of chronic liver disease and focal lesions demonstrated good agreement between conUS and 3DUS (**see Supplement 4 for details**).

Figure 4 provides an overview of the stitched 3DUS images in the patient cohort. **Panel 4A** shows a focal nodular hyperplasia (FNH) lesion captured using two volumes, with the stitching line running through the lesion to assess proper volume alignment. The stitched volumes (**Figure 4A**) clearly depict the lesion with an precise diameter. **Figure 4B** illustrates a small hyperechoic hemangioma visible in all three imaging planes of good quality. Differences in echogenicity between the liver and renal parenchyma are apparent in the stitched volume (**Figure 4C),** and the irregular liver surface in cirrhosis patients is evident in **Figure 4D**. Even for focal lesions located directly within the overlapping stitching zone, the diagnostic accuracy remained high (89% for FNH and 95% for hemangioma). As an example, **Figure 5** illustrates how overlapping 3D volumes of an FNH lesion were recorded; the final stitched result shows a precise overlap and a clearly demarcated lesion. In comparison, 3DUS visualization of chronic liver disease morphology was somewhat inferior to that of focal lesions, especially in terms of assessing the liver margin in patients with chronic liver disease.

3DUS-specific artifacts

The merging of multiple adjacent volumes inevitably introduces image artifacts arising from various factors. Four main types of artifacts were identified: **A)** artifacts that arise from the acquisition of a 3D volume, such as those due to different transducer pressures, different breathing commands, or pulsation artifacts**. B)** Artifacts caused by deviation of the scanning movement (“folding artifacts”) that occur due to different speeds of transducer movement in the inner and outer areas of the acquisition. **C)** Stitching artifacts related to the superimposition of one or more volumes. **D)** Artifacts known from conventional ultrasound (conUS) that now appear combined from multiple insonation angles (e.g., acoustic enhancement or shadowing).

Artifacts vary in severity depending on the chosen scan mode and trajectory. Straight scan paths showed minimal folding artifacts (This effect can be illustrated by Scan 5, which consists of three parallel transverse slices acquired directly adjacent to each other with minimal overlap of only a few centimeters; see Supplementary Material 1). In contrast, folding artifacts increased when the volumes were angled relative to each other or when the scan path was curved (Scan 1 comprised a total of four adjacent acquisitions, with two scans obtained in the sagittal plane and two in a modified transverse plane; see Supplementary Material 1). Pulsation artifacts mainly occurred in the sagittal scans (Sans 1, 3, 4, and 6, see Supplementary Material 1) because heart motion and breathing caused stronger shifts between images.

Stitching artifacts can be mitigated through automated rigid volume postprocessing, a feature integrated into 3DUS device software. **Figure 4E and 4F** illustrate an example of a stitched volume with a portal vein segment before and after postprocessing. Prior to postprocessing (**Figure 4E**), the portal vein appeared discontinuous due to folding artifacts. After rigid volume postprocessing (**Figure 4F**), the continuity of the portal vein markedly improved.

Exemplary use cases for 3DUS

To demonstrate a potential use case for 3D ultrasound tomography, a comprehensive human liver and neonatal ultrasound phantom was scanned via the 3DUS technique. The results showed that a complete scan of an entire human liver (**Supplement 5**) and an even more an entire (neonatal) body is technically feasible with promising image quality (see **Figure 2B and Supplement 6**).

Additionally, in an exploratory application, an adult human torso was scanned in three stitched volumes. While the image quality was affected by artifacts, as expected, the general result was satisfactory. As shown in **Figure 6**, a complete depiction of the human torso was achieved, encompassing the entire abdomen, from the diaphragm and the full length of the aorta to the bladder, with acceptable image quality.

Both tomographic datasets could be analysed via multiplanar reconstruction in any desired plane, enabling retrospective image review independent of the examiner. The dataset could also be utilized for automated image analysis and reconstruction, such as automatic segmentation of the bladder.

Discussion

For decades, abdominal ultrasound diagnostics have been limited by the restricted field of view, which has hindered the comprehensive visualization of large organs and entire anatomical compartments [22]. Our findings indicate that tomographic three-dimensional ultrasound acquisition combined with multiscan stitching may help to overcome these constraints and could enable standardized assessments of larger abdominal structures, including retrospective and examiner-independent image review [13,23,24].

These results align conceptually with prior work in 3D ultrasound mosaicing/compounding across cardiac, foetal, and breast imaging, which demonstrated preserved or improved geometric fidelity and image quality after multi-view fusion (15–18). However, our setting differs materially due to deep abdominal anatomy, respiratory motion, and the use of convex probes. These factors likely explain the observed trade-off between increased field of view and perceived image quality compared with 2D conUS.

The pilot data from healthy volunteers demonstrate that the use of 3D sonography is technically feasible for large abdominal regions and can be performed with convincing image quality under favourable examination conditions. Conventional ultrasound (conUS) served as the reference standard for image quality assessment in 3D ultrasound (3DUS). For methodological reasons, the image quality of 3DUS cannot exceed that of the underlying B-mode acquisitions. Moreover, image quality declined in our experiments with an increasing number of stitched volumes and with higher acquisition complexity, indicating that degradation arises both from the recording strategy, such as straight versus oblique probe movements, and from cumulative stitching-related artifacts.

Although a reduction in image quality was observed in the reconstructed 3D volumes, this feasibility study was not designed to quantify the downstream impact on diagnostic performance or clinical decision-making. In particular, the effect on diagnostic confidence and sensitivity for subtle findings remains uncertain and will require dedicated diagnostic accuracy studies with an appropriate reference standard.

To further evaluate the feasibility of potential clinical applications, additional examinations were conducted on patients with liver diseases. In the stored 3D datasets, characteristic markers of parenchymal liver diseases, such as irregular liver surfaces and heterogeneous liver parenchyma, were clearly visualized. We also investigated the potential of 3D imaging for focal liver lesions a particularly relevant application for monitoring the progression of abdominal metastases, where conventional ultrasound often shows limited diagnostic sensitivity [25]. Even lesions situated at the interface of overlapping volumes were clearly delineated. In focal lesions crossing stitch interfaces, lesion diameter and margin continuity remained stable across planes, supporting the geometric consistency of the reconstructed datasets. Nevertheless, controlled geometric validation against an external ground truth, such as CT-derived surfaces or centrelines in phantoms or selected clinical cases, would be required to provide objective accuracy bounds for 3DUS and should be prioritized in next-step studies

Another possible application of abdominal 3D ultrasound approaches lies in rural healthcare settings or prehospital emergency scenarios, such as trauma diagnostics, where local ultrasound expertise may be unavailable. In these situations, standardized 3D datasets could be transmitted via telemedicine for specialist review [26,27]. To assess the feasibility of

complete abdominal imaging, we initially scanned a neonatal ultrasound torso. The resulting images demonstrated excellent quality and highlighted the technical capabilities of this approach under phantom conditions. To simulate a more realistic clinical environment with intestinal gas interference, we subsequently performed a full abdominal scan on a healthy adult volunteer. The image quality remained satisfactory, allowing visualization of major abdominal organ systems. However, this adult torso scan should be only interpreted as a proof-of-concept example and not as evidence of diagnostic accuracy, since it was not quantitatively evaluated.

Our data on large-scale abdominal 3D ultrasound applications build on earlier studies that demonstrated the feasibility of stitching multiple adjacent 3D ultrasound volumes for superficial structures using linear transducers [16,28]. We demonstrated that a similar technique is also viable for abdominal imaging with more technically complex convex probes and disturbances caused by breathing, organ motion, and intestinal gas interference. While these findings underscore the technical viability of 3DUS, they also reveal limitations arising from these interfering factors.

Our results emphasize several technical considerations necessary for the routine clinical implementation of 3DUS. First, the quality of the reconstructed 3D dataset strongly depends on the quality of the underlying B-mode ultrasound images [29]. Consequently, the use of state-of-the-art ultrasound equipment with optimized imaging parameters is crucial. Ultrasound image quality is strongly influenced by external conditions, making it susceptible to various artifacts and disturbances arising from the physical properties of ultrasound transmission and reflection. In this study, imaging parameters were optimized primarily for diagnostic B-mode image quality, consistent with routine clinical ultrasound practice. However, the optimal parameter set for automated stitching may differ from visually optimized settings, because registration algorithms may benefit from standardized gain, dynamic range, depth, focus, and time-gain compensation settings across all sub-volumes. These parameters were not systematically varied in the present feasibility study and should therefore be addressed in future protocol optimization studies.

Second, tracking systems play a pivotal role in the accuracy of volume registration. In the present study, magnetic tracking was employed, but it is susceptible to interference from external magnetic fields and metallic structures, such as the examination table [30]. Although the electromagnetic tracking subsystem provides sub-millimetre positional accuracy under idealized conditions, the actual tracking accuracy in the clinical examination environment was not independently quantified in this study. Field distortions caused by metallic structures, nearby equipment, or changes in the relative position of the field generator and transducer may propagate into the reconstructed 3D volume as spatial misregistration, seam discontinuity, or local geometric distortion, particularly in overlap regions. Future validation studies should therefore include environment-specific tracking calibration and phantom-based error measurements under realistic clinical room conditions. Alternative tracking methods, including optical systems or relative positioning detection via gyroscopes, may overcome some of these shortcomings and further reduce artifacts [31–33]. In simulator-based ultrasound education settings, optical tracking systems are already being used with convincing results [17]. Tracker-less approaches based on image-based registration and/or learning-based pose estimation, widely explored in other anatomies, such as cardiac echocardiography and breast, may further simplify deployment by removing external sensors [18,19].

In recent years, technical advances in ultrasound hardware and image software processing have significantly progressed [13,23], making the routine clinical use of 3DUS increasingly feasible. However, the present study also revealed that there are still deficits in image quality compared with conventional B-mode imaging. With continued technological advancements and mitigation of artifacts, 3DUS could provide standardized anatomical presentations in multiple planes, similar to those of CT or MRI, in selected routine clinical applications in the future.

In addition to the technical challenges of 3DUS, acquisition-related problems exist in the registration of volumetric datasets. Diagnostic ultrasound benefits from dynamic images, whereas the registration of a larger 3DUS scan produces a static record. This is particularly relevant for examinations requiring continuous assessment over time, such as vascularity assessment using Doppler ultrasound and especially contrast-enhanced ultrasound, where static recording may impose meaningful diagnostic limitations. A potential mitigation strategy, analogous to cross-sectional imaging, could be to repeat

acquisitions at several predefined time points. However, continuous four-dimensional acquisition with an explicit temporal component is currently achievable only using 4D matrix transducers.

In addition, the acquisition of ultrasound images, particularly in liver imaging, often benefits from deep patient inspiration or left lateral positioning to enhance parenchymal visualization [34]. During volumetric registration, inevitable changes and deformations in human anatomy occur due to pulsation artifacts, inspiration, or transducer pressure causing deformation of the underlying organs, leading to deformation artifacts [15,35]. Rigid registration can correct global pose differences, while deformable models can absorb local non-rigid effects [36]; however, over-fitting risks must be controlled via regularization and validation on anatomical landmarks. Otherwise, there is a risk that the initial metric volumetric dataset could become distorted, resulting in less accurate measurements.

To address such issues, rigid registration algorithms can correct plane displacement via rotation and translation [37], whereas deformable algorithms allow the adaptation of structures within individual planes to account for more complex distortions [38,39]. However, even with the use of various optimization algorithms, acquiring 3DUS datasets in sonographically challenging regions, such as liver segment VII with ribs and air in the ultrasound path, can remain challenging. Since the applied registration and stitching workflow was implemented in a commercial software environment, full algorithmic reproducibility is limited. This should be considered when interpreting the results and when comparing them with future implementations or alternative systems.

This study was designed as a pilot investigation to explore the utility of the specific 3DUS system used. Consequently, it has inherent limitations, including a small sample size of both patients and healthy volunteers, evaluation restricted to one 3DUS platform using an ordinal scale, and the absence of inter- and intra-observer reliability measures. Furthermore, the results are inherently dependent on the specific system configuration used, including the ultrasound scanner, curved-array transducer, electromagnetic tracking system, acquisition presets, scan trajectory, overlap width, and postprocessing software. Moreover, the phantom and patient cohorts were selected to represent technically favourable conditions and do not cover the full range of clinical variability, such as obesity, severe meteorism, limited acoustic windows, postoperative anatomy, or highly mobile target organs. Quantitative assessment of lesion dimensions demonstrated satisfactory accuracy, although detailed quantification studies remain necessary. In particular, the present study did not include a dedicated quantitative assessment of volumetric accuracy in all three spatial dimensions or along the scan direction

Despite the technical limitations of 3D imaging and the study-related constraints of a pilot project, this investigation demonstrated that large-scale abdominal ultrasound imaging is feasible with the current state of technology under selected and favourable conditions. Moreover, convincing sonographic image data were generated.

The exploratory acquisition of a complete adult abdominal scan illustrates the potential of this approach but should not be interpreted as proof of general diagnostic reliability. This important development may open a wide range of new applications for ultrasound imaging. For example, this technology could help integrate ultrasound more firmly into multidisciplinary tumour board presentations, as it enables retrospective re-interpretation of imaging data. In addition, such large-volume ultrasound datasets could serve as a basis for training AI-supported image analysis tools.

The present study should therefore be interpreted strictly as a feasibility and workflow study rather than as a quantitative validation of geometric accuracy or diagnostic performance. The findings demonstrate that large-volume abdominal 3DUS stitching is technically feasible under controlled and favourable clinical conditions, but they do not yet define generalizable accuracy limits for broader clinical use.

In summary, our study results highlight the technical feasibility of large-scale abdominal ultrasound imaging while identifying limitations that are likely to may be resolved with future technological advancements. Particularly in the context of automated image analysis and diagnostic algorithms, high-resolution and reproducible imaging investigations hold significant medical relevance. The concept of remote expert evaluation, particularly in resource-limited settings, is

compelling. However, robustness and reliability data from inexperienced operators are lacking and must be demonstrated in future studies.

Future research should focus on refining acquisition protocols, harnessing advanced computational algorithms, including artificial intelligence, for artifact reduction and improved stitching, and integrating 3D functionalities into ultrasound systems to increase usability and diagnostic precision. Furthermore, validation studies with larger and more diverse patient cohorts, including patients with malignancies, obesity, meteorism, and impaired acoustic windows, are needed. To our knowledge, this is the first study specifically evaluating the potential of 3DUS in an abdominal context, paving the way for further investigations and clinical translation.

In conclusion, tomographic acquisition and multiscan stitching of abdominal ultrasound images are technically feasible in phantoms and selected patients and may enable retrospective review of standardized large-volume datasets. However, the current results remain exploratory and system-specific. Quantitative validation of geometric accuracy, robustness under realistic clinical conditions, and diagnostic performance is required before broader clinical implementation.

Conclusion

This pilot study demonstrates that tomographic three-dimensional abdominal ultrasound combined with multiscan stitching is technically feasible for generating large-volume, standardized ultrasound datasets in phantoms, healthy volunteers, and selected patients with liver disease. Under controlled and favourable examination conditions, adjacent 3D ultrasound volumes could be successfully merged, enabling retrospective multiplanar review and examiner-independent assessment of abdominal anatomy. In healthy volunteers, the technique allowed large-area liver and abdominal organ coverage, while in patients it enabled visualization of focal liver lesions as well as characteristic features of chronic parenchymal liver disease. The phantom and proof-of-concept torso examinations further illustrate the potential of this approach for standardized training, telemedical review, and future automated image analysis.

The importance of this study lies in addressing a central limitation of conventional abdominal ultrasound: its restricted field of view and operator-dependent documentation. By creating comprehensive 3D datasets that can be reviewed after acquisition, multiscan 3DUS may help bridge the gap between conventional ultrasound and cross-sectional imaging, particularly for follow-up examinations, tumour board presentations, remote expert assessment, and AI-supported diagnostic workflows.

However, the results must be interpreted as exploratory. Image quality remained dependent on the underlying B-mode acquisition and was reduced by acquisition complexity, respiratory motion, tracking limitations, and stitching-related artifacts. The study was limited by its small and selected cohort, the use of a single commercial 3DUS platform, and the absence of quantitative validation against an external reference standard. Therefore, future studies should assess geometric accuracy, diagnostic performance, interobserver reliability, and robustness in larger and more heterogeneous patient populations before broader clinical implementation can be recommended.

Overall, multiscan tomographic 3D ultrasound represents a promising step toward standardized, reproducible, and retrospectively assessable abdominal ultrasound imaging, while clearly identifying the technical and clinical validation steps required for translation into routine practice.

Abbreviations

3DUS — Three-dimensional ultrasound

4D — Four-dimensional

AI — Artificial intelligence

BMI — Body mass index

CE — Conformité Européenne

conUS — Conventional ultrasound

CT — Computed tomography

DRKS — German Clinical Trials Register

FAST — Focused Assessment with Sonography for Trauma

FNH — Focal nodular hyperplasia

HDMI — High-Definition Multimedia Interface

MASLD — Metabolic dysfunction-associated steatotic liver disease

MRI — Magnetic resonance imaging

POCUS — Point-of-care ultrasound

ROI — Region of interest

US — Ultrasound

Declarations

Acknowledgements

We thank the company PIUR IMAGING GmbH (Vienna, Austria) for their technical support. We further acknowledge support from Leipzig University for Open Access Publishing.

Author contribution

All authors (VB, PS, JW, TK) contributed equally to study design, data curation, formal analysis, interpretation, manuscript drafting and critical revision, and approved the final version of the manuscript. Patient examinations were performed by VB and PS.

Data Availability Statement.

The datasets are available from the corresponding author on reasonable request.

Funding

This work was supported by the Federal Ministry of Education and Research (BMBF) through a MetaRot Grant from the Integrated Research and Treatment Center AdiposityDiseases Leipzig (IFB), Germany, FKZ01EO1001. The funders had no role in the study design, data collection and analysis, decision to publish, or preparation of the manuscript.

Ethics approval and consent to participate

This study was conducted in accordance with the ethical principles of the Declaration of Helsinki and the guidelines for Good Clinical Practice (ICH-GCP E6/R1). The study was approved by the local ethics committee of the University of Leipzig, Leipzig, Germany (approval/registration number: 059/19-ek). All human participants provided written informed consent to participate before inclusion in the study.

Declaration of interests

Valentin Blank reports financial support was provided by Federal Ministry of Education and Research (BMBF). We thank the company PIUR IMAGING GmbH (Vienna, Austria) for their technical support. If there are other authors, they declare that they have no known competing financial interests or personal relationships that could have appeared to influence the work reported in this paper.

Paula Schwabe, Johannes Wiegand and Thomas Karlas declare that they have no known competing financial interests or personal relationships that could have appeared to influence the work reported in this paper.

Clinical trial registration

The study was registered in the German Clinical Trials Register (DRKS; registration number: DRKS00016736; registration date: 27.05.2019).

Declaration of generative AI and AI-assisted technologies in the writing process

During the final preparation of this work, the author used ChatGPT (ChatGPT-5.5) to assist only with language refinement, grammar editing, and improvement of academic phrasing in English. After using this tool, the author thoroughly reviewed and edited the content to ensure accuracy and takes full responsibility for the content of the publication.

References

1. Moore CL, Copel JA. Point-of-Care Ultrasonography. N Engl J Med. 2011;364:749–57.
2. Bitzer M, et al. S3-Leitlinie „Diagnostik und Therapie des Hepatozellulären Karzinoms – Langversion 4.0. Z Gastroenterol. 2024;62:e67–161.
3. Beyer G, et al. S3-Leitlinie Pankreatitis – Leitlinie der Deutschen Gesellschaft für Gastroenterologie, Verdauungs- und Stoffwechselkrankheiten (DGVS) – September 2021 – AWMF Registernummer 021 – 003. Z Gastroenterol. 2022;60:419–521.
4. Heese F, Görg C. Diagnostische Wertigkeit einer internistischen Referenzsonographie (DEGUM-Stufe 3). Ultraschall Med. 2006;220–4. 10.1055/s-2006-926665.
5. Education and Practical Standards Committee. European Federation of Societies for Ultrasound in Medicine and Biology. Minimum training recommendations for the practice of medical ultrasound. Ultraschall Med. 2006;27:79–105.
6. De Muzio F, et al. CT study protocol optimization in acute non-traumatic abdominal settings. Eur Rev Med Pharmacol Sci. 2022;26:860–78.
7. Yi J, et al. Technology trends and applications of deep learning in ultrasonography: image quality enhancement, diagnostic support, and improving workflow efficiency. Ultrasonography. 2021;40:7–22.
8. Tanabe K. Three-Dimensional Echocardiography — Role in Clinical Practice and Future Directions —. Circ J. 2020;84:1047–54.
9. Leung K-Y. Applications of Advanced Ultrasound Technology in Obstetrics. Diagnostics (Basel). 2021;11:1217.
10. Fenster A, Downey DB, Cardinal H. N. Three-dimensional ultrasound imaging. Phys Med Biol. 2001;46:R67–99.
11. Nelson TR, Pretorius DH. Three-dimensional ultrasound imaging. Ultrasound Med Biol. 1998;24:1243–70.
12. Prager RW, Ijaz UZ, Gee AH, Treece GM. Three-dimensional ultrasound imaging. Proc Inst Mech Eng H. 2010;224:193–223.
13. Blank V, Wiegand J, Keim V, Karlas T. Evaluation of a novel tomographic ultrasound device for abdominal examinations. PLoS ONE. 2019;14:e0218754.
14. Alzahrani A, Alotaibi SA, Aslam M, Sultan SR. Reliability and Accuracy of Tomographic 3-D Ultrasound for Grading Vessel Stenosis: A Phantom Study. Ultrasound Med Biol. 2022;48:1899–906.

15. Gee AH, Treece GM, Prager RW, Cash CJC, Berman L. Rapid registration for wide field of view freehand three-dimensional ultrasound. IEEE Trans Med Imaging. 2003;22:1344–57.
16. Freesmeyer M, Knichel L, Kuehnel C, Winkens T. Stitching of sensor-navigated 3D ultrasound datasets for the determination of large thyroid volumes - a phantom study. Med Ultrason. 2018;20:480–6.
17. Lucius C, et al. [State of the art: Simulation in US]. Z Gastroenterol. 2024;62:723–36.
18. Perperidis A. Postprocessing Approaches for the Improvement of Cardiac Ultrasound B-Mode Images: A Review. IEEE Trans Ultrason Ferroelectr Freq Control. 2016;63:470–85.
19. Wachinger C, Wein W, Navab N. Registration strategies and similarity measures for three-dimensional ultrasound mosaicing. Acad Radiol. 2008;15:1404–15.
20. Wright R, et al. Fast fetal head compounding from multi-view 3D ultrasound. Med Image Anal. 2023;89:102793.
21. Ortiz SHC, Macione J, Chiu T, Fox MD. Super-resolution of ultrasound images by displacement, averaging, and interlacing. in *Medical Imaging 2009: Ultrasonic Imaging and Signal Processing* vol. 7265 391–398 (SPIE, 2009).
22. Rizzatto G. Ultrasound transducers. Eur J Radiol. 1998;27:S188–95.
23. Fritz GA, Riccabona M, Bohdal G, Quehenberger F. Nierenvolumetrie im Kindesalter: Genauigkeit der dreidimensionalen Sonographie im Vergleich zur konventionellen Sonographie und CT / MRT. Rofo. 2003;175:540–6.
24. Downey DB, Fenster A, Williams JC. Clinical utility of three-dimensional US. Radiographics. 2000;20:559–71.
25. Cantisani V, et al. Liver metastases: Contrast-enhanced ultrasound compared with computed tomography and magnetic resonance. World J Gastroenterology: WJG. 2014;20:9998.
26. Kleemann T, et al. Proof of Concept of Telemedicine-Assisted Abdominal Ultrasound Examinations to Improve the Quality of Patient Care in Rural Areas. J Clin Med. 2024;13:1721.
27. Duan S, et al. A 5G-powered robot-assisted teleultrasound diagnostic system in an intensive care unit. Crit Care. 2021;25:134.
28. Seifert P, Winkens T, Knichel L, Kühnel C, Freesmeyer M. Stitching of 3D ultrasound datasets for the determination of large thyroid volumes - phantom study part II: mechanically-swept probes. Med Ultrason. 2019;21:389–98.
29. Hung ALY, Galeotti J. Good and bad boundaries in ultrasound compounding: preserving anatomic boundaries while suppressing artifacts. Int J Comput Assist Radiol Surg. 2021;16:1957–68.
30. Fenster A, Parraga G, Bax J. Three-dimensional ultrasound scanning. Interface Focus. 2011;1:503–19.
31. Prager RW, Ijaz UZ, Gee AH, Treece GM. Three-dimensional ultrasound imaging. Proc Inst Mech Eng H. 2010;224:193–223.
32. Chan VS, et al. Using game controller as position tracking sensor for 3D freehand ultrasound imaging. Med Biol Eng Comput. 2020;58:889–902.
33. Herickhoff CD, Morgan MR, Broder JS, Dahl JJ. Low-cost Volumetric Ultrasound by Augmentation of 2D Systems: Design and Prototype. Ultrason Imaging. 2018;40:35–48.
34. Kremkau FW, Taylor KJ. Artifacts in ultrasound imaging. J Ultrasound Med. 1986;5:227–37.
35. Fenster A, Downey DB, Cardinal H. N. Three-dimensional ultrasound imaging. Phys Med Biol. 2001;46:R67.
36. Rueckert D, et al. Nonrigid registration using free-form deformations: application to breast MR images. IEEE Trans Med Imaging. 1999;18:712–21.
37. Che C, Mathai TS, Galeotti J. Ultrasound registration: A review. Methods. 2017;115:128–43.
38. Figl M, Hoffmann R, Kaar M, Hummel J. Deformable registration of 3D ultrasound volumes using automatic landmark generation. PLoS ONE. 2019;14:e0213004.
39. Mao Z, et al. Complete region of interest reconstruction by fusing multiview deformable three-dimensional transesophageal echocardiography images. Med Phys. 2023;50:61–73.
40. Seitzinger M, et al. Development, evaluation, and overview of standardized training phantoms for abdominal ultrasound-guided interventions. Ultraschall Med. 2024;45:176–83.

41. Mori T, Nomura O, Takei H, Fukuhara S, Ichihashi K. Implementation and assessment of a pediatric point-of-care ultrasound training course in Japan: a pilot study. *J Med Ultrason (*2001) 49, 85–93 (2022).
42. Pediatric FASTA. Abdomen Phantom | KYOTO KAGAKU. https://www.kyotokagaku.com/en/products_data/us-8/
43. Rogers SK, et al. Feasibility and Accuracy of Measuring Carotid Plaque Volume (Burden) With Contrast-Enhanced Tomographic 3D Ultrasound and Ultrasound Image Fusion. Ann Vasc Surg. 2023;91:168–75.
44. Krönke M, et al. Tracked 3D ultrasound and deep neural network-based thyroid segmentation reduce interobserver variability in thyroid volumetry. PLoS ONE. 2022;17:e0268550.
45. Chan YC, Cheung GC, Cheng SW. Tomographic three-dimensional ultrasound imaging improves spatial visualization and management of varicose veins. *jvascsurgc* 10, (2024).

Tables

Table 1 Baseline characteristics and comparison of image quality and completeness.

	Healthy volunteers	**Patients**				
		Total patients	**FNH**	**Haemangioma**	**Cirrhosis**	**MASLD**
Numbers	22	22	5	7	5	5
females (%)	11 (50%)	15 (68%)	4 (80%)	5 (71%)	3 (60%)	3 (60%)
Age [years]	24.9 ± 8.1	45.7 ± 14.5	30.2 ± 14.4	48.9 ± 6.4	47.4 ± 15.5	55 ± 8.6
BMI [kg/m²]	21.1 ± 1.4	24.7 ± 5.2	20.3 ± 2.2	26.8 ± 3.7	25.1 ± 5.7	26 ± 5.9
< 18.5	0 (0%)	4 (18%)	2 (40%)	0 (0%)	1 (20%)	1 (20%)
18.5 - 24.9	22 (100%)	8 (36%)	3 (60%)	3 (43%)	1 (20%)	1 (20%)
25 - 30	0 (0%)	5 (23%)	0 (0%)	2 (29%)	2 (40%)	1 (20%)
> 30	0 (0%)	5 (23%)	0 (0%)	2 (29%)	1 (20%)	2 (40%)
Duration conUS [min]	15.9 ± 4	15 ± 5.7	13.4 ± 3.8	13.7 ± 3.9	17.4 ± 5.3	16.2 ± 8.3
Duration 3DUS [min]	15.7 ± 3.6	10.9 ± 4.2	13.4 ± 4.5	9.9 ± 2.7	10.8 ± 3.7	9.8 ± 4.8
Image quality (all scans)	74%	81%	82%	80%	75%	87%
Organ covering (all scans)	74%	70%	72%	64%	76%	74%
Delimination of lesions (quality of visualization)	NA	NA	100%	95%	NA	NA
Characterization of liver parenchyma (quality)	71%	77%	85%	64%	76%	92%

FNH = focal nodular hyperplasia, MASLD = metabolic-associated steatotic liver disease, BMI = body mass index; conUS = conventional ultrasound. 3DUS = three-dimensional ultrasound. Number (percent). Average ± standard deviation.

Figures

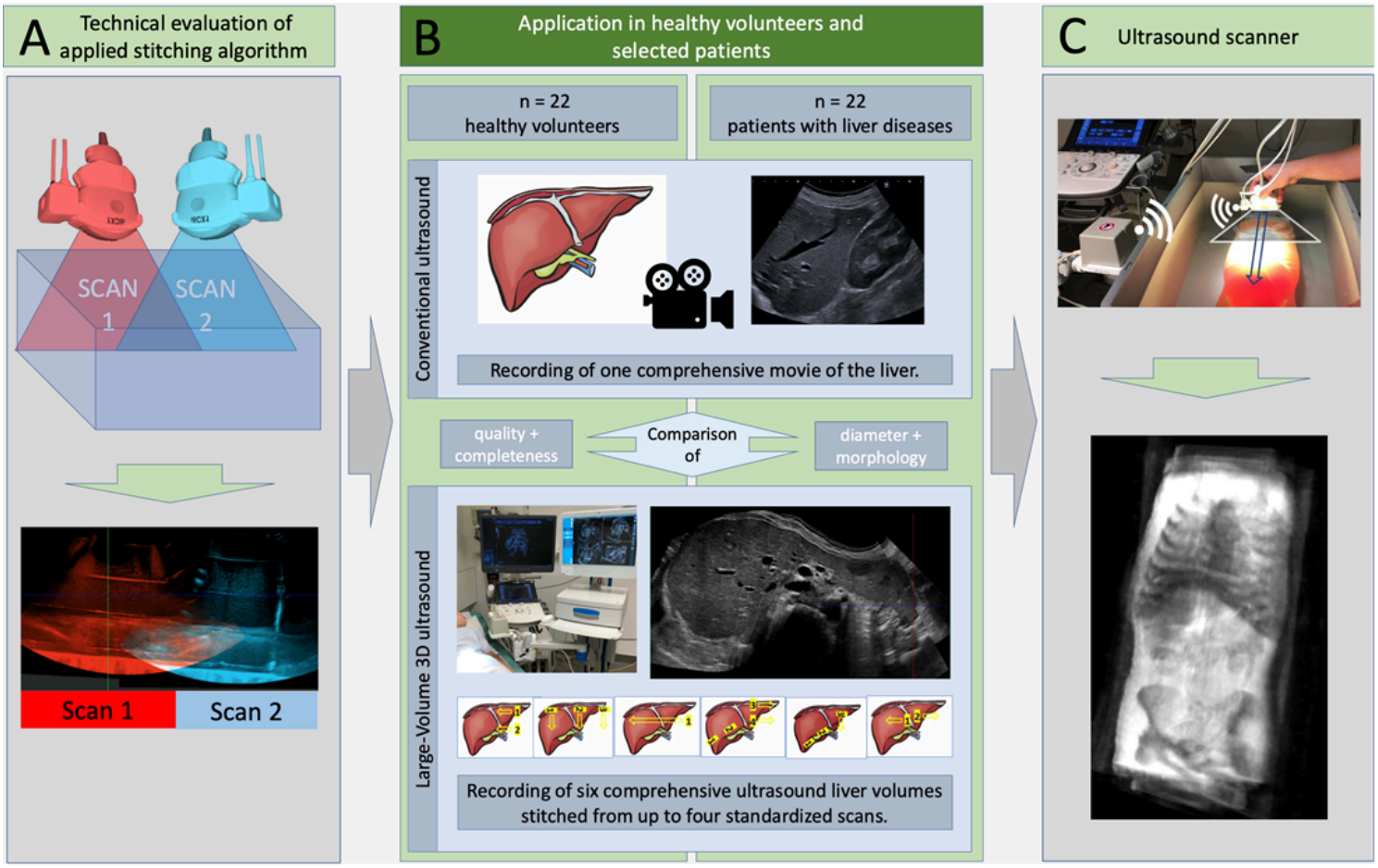

Figure 1

Study design.

A Technical Evaluation: Assessment of a novel stitching algorithm for adjacent ultrasound volumes. **B** Prospective study: Evaluation of the technical feasibility, image quality, and completeness of stitched large-area tomographic ultrasound volumes in an abdominal setting, using conventional ultrasound as a reference in healthy volunteers and patients with focal or chronic liver diseases. **C**Prototype Testing: Evaluation of an ultrasound tomograph prototype using a pediatric ultrasound phantom immersed in water.

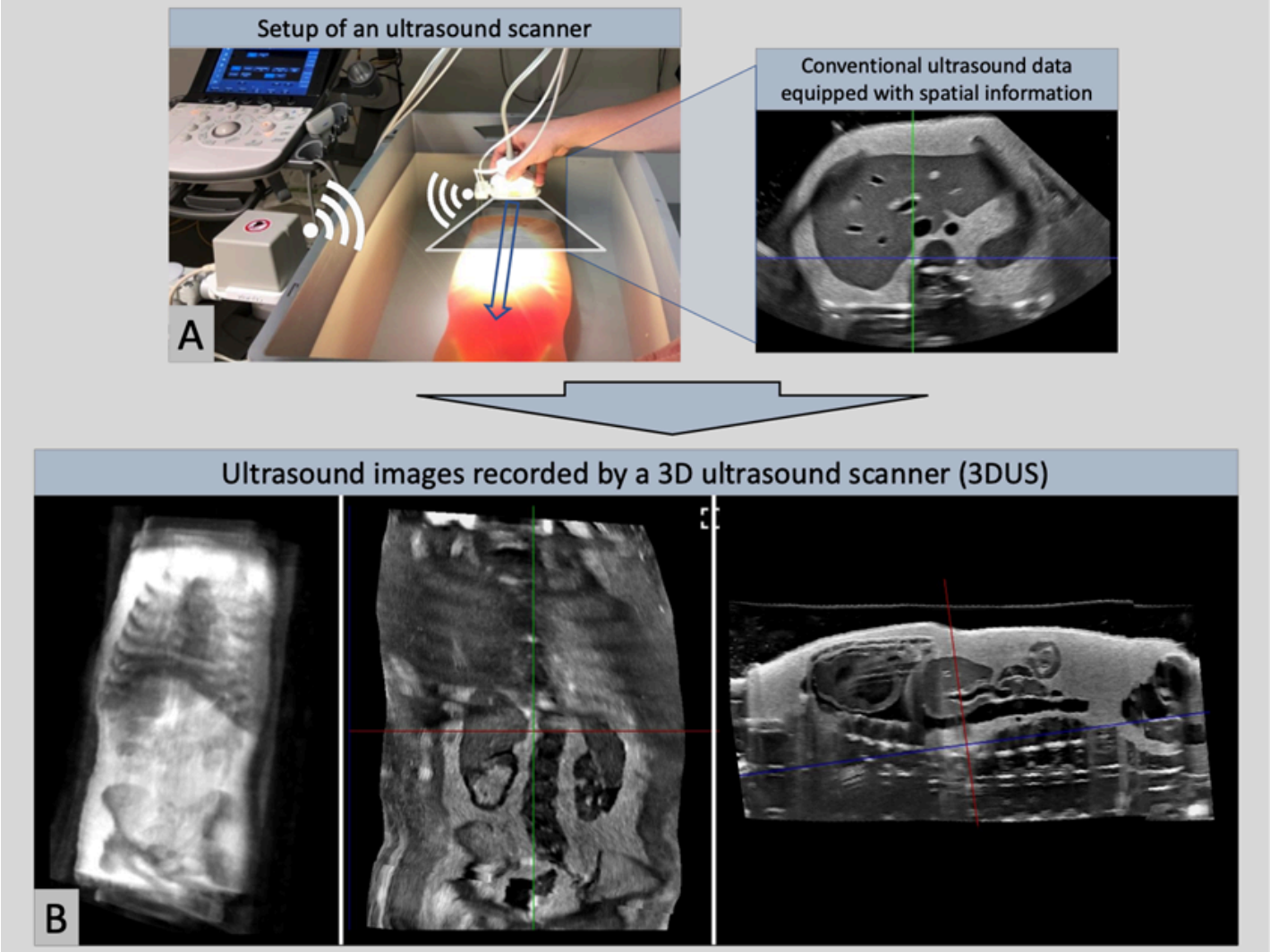

Figure 2

Setup and tomographic ultrasound images of a tomographic ultrasound scanner.

A Setup: The tomographic 3D ultrasound system integrates a conventional ultrasound probe with a magnetic field tracking system, enabling spatial information to be linked to the digital video output of a standard ultrasound machine.
BTomographic ultrasound images: Left – a topogram of the ultrasound volume generated from a neonatal ultrasound phantom. Middle – frontal plane. Right – the sagittal plane.

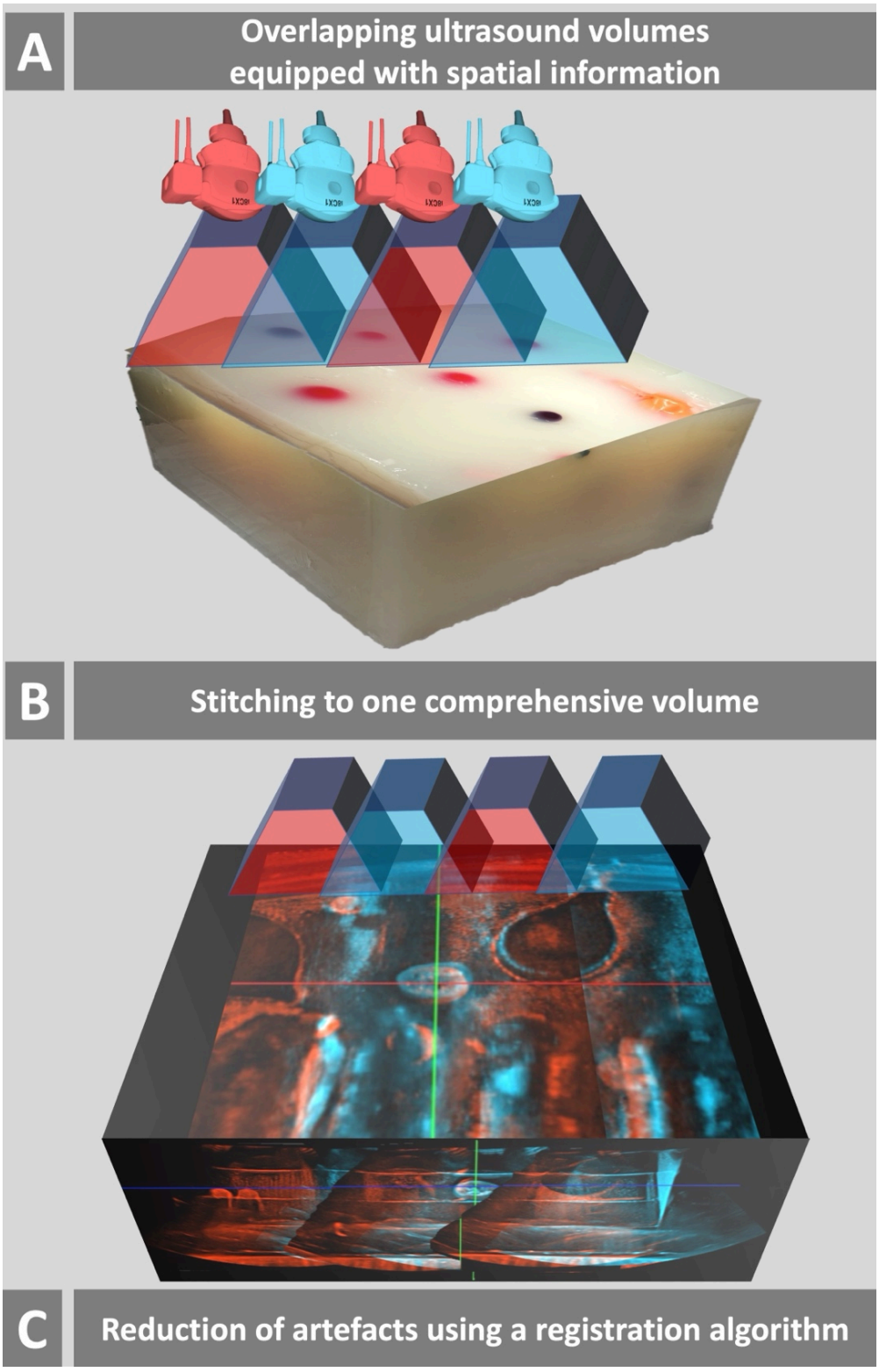

Figure 3

Principle of an ultrasound-based switching algorithm using Multiscan technology.

A Technical Evaluation: A standardized ultrasound phantom with predefined lesions was used to evaluate the stitching algorithm and identify stitching artifacts. The ultrasound transducer, equipped with a magnetic tracking system, was moved four times over the phantom in parallel paths, with an overlapping area of 2–3 cm between adjacent volumes. **B**Volume Stitching: The four partially overlapping ultrasound volumes were combined into a single comprehensive volume, with

overlapping data suppressed. **C**Postprocessing: Registration techniques were applied during postprocessing to minimize artifacts.

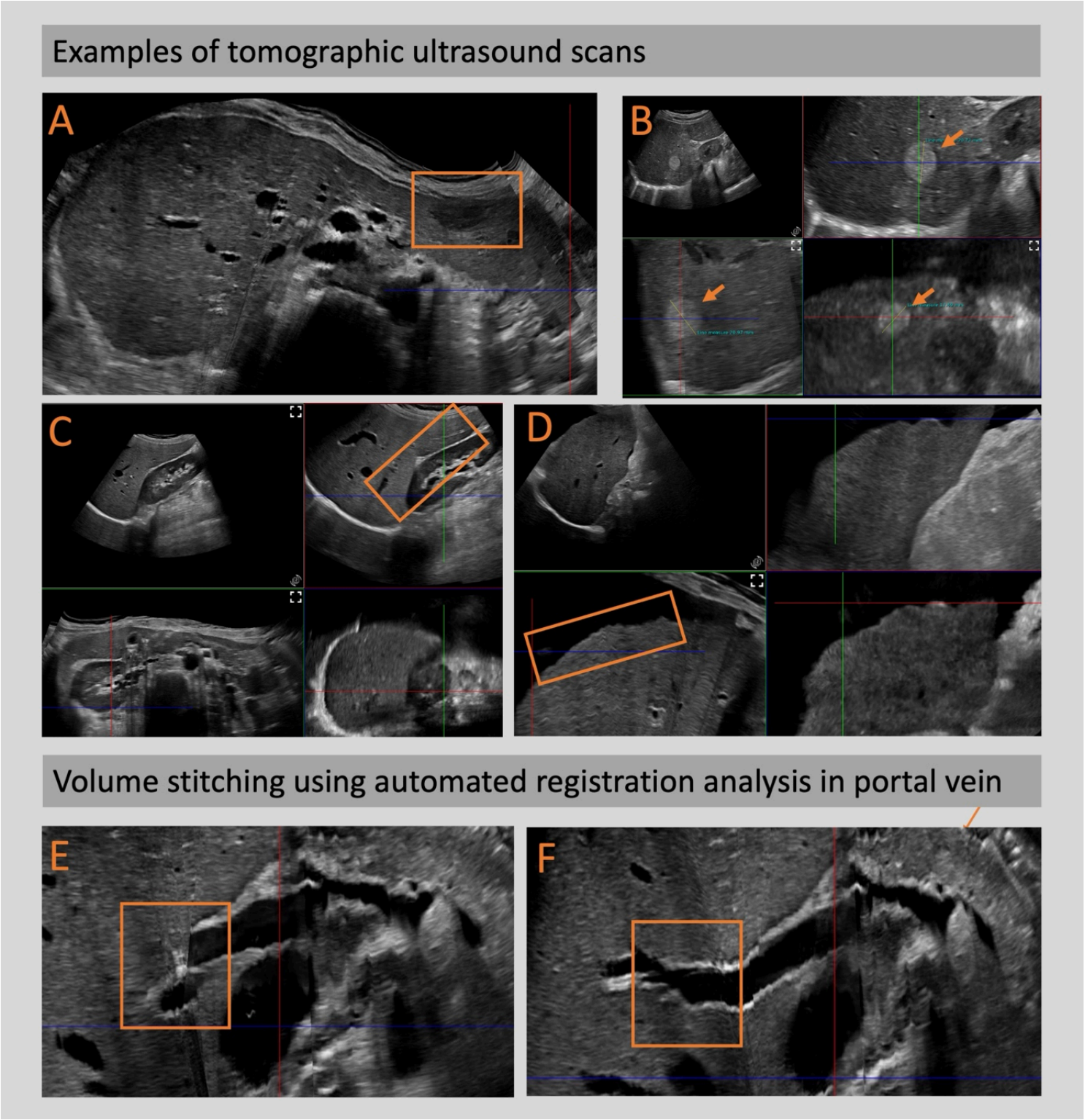

Figure 4

Examples of tomographic ultrasound images and results of the rigid registration algorithm

A Focal Nodular Hyperplasia: Depicted as a hypoechoic focal lesion within a comprehensive volume of the entire liver. **B.** Hemangioma: a hyperechoic focal lesion visualized in all three planes. **C**. Fatty liver disease: the contrast between the hyperechogenic liver parenchyma and the parenchyma of the right kidney is clearly visible. **D**. Liver cirrhosis: Visualization of

an irregular liver surface, a morphological characteristic of cirrhosis. **E.**Volume registration algorithm: Left – before automated registration; right – afterautomated registration. Portal vein alignment was successfully improved through the registration process.

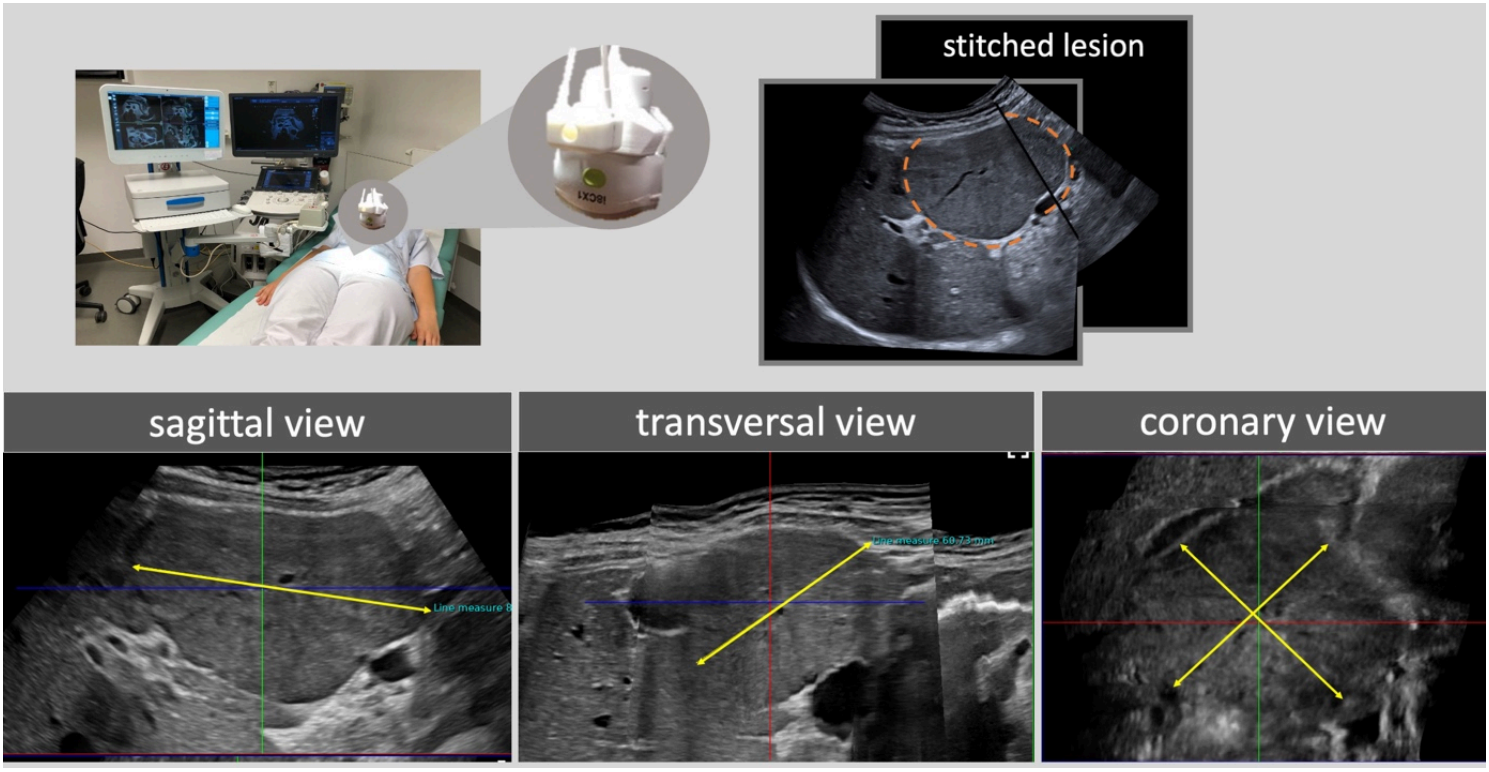

Figure 5

Comprehensive tomographic ultrasound data of a large liver lesion

Top Left: Setup of the workstation, including a conventional ultrasound scanner and a technical workstation that integrates spatial information into the conventional ultrasound data. **Top right**: Conventional ultrasound images depicting the large liver lesion, displayed across two side-by-side scans. **Bottom:**Exemplary representation of the stitched tomographic ultrasound data, visualized in the sagittal, transverse, and coronal planes.

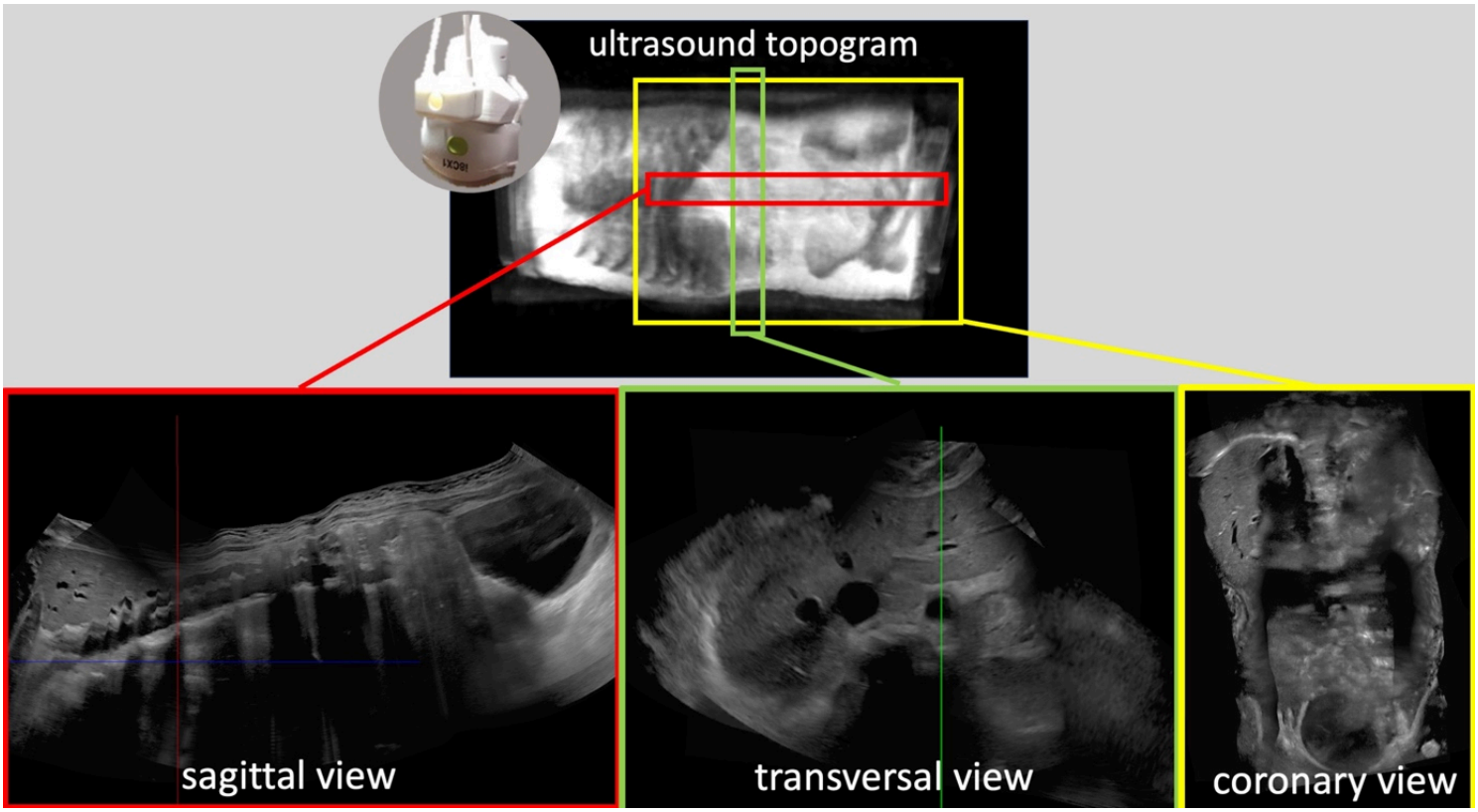

Figure 6

Tomographic ultrasound image of a comprehensive adult abdominal scan.

Top left: Workstation setup featuring a conventional ultrasound scanner and a technical workstation for integrating spatial information into conventional ultrasound data. **Top right:** Conventional ultrasound data enhanced with spatial information from video output. **Bottom:** Example of the calculated tomographic ultrasound data displayed in the sagittal, transverse, and coronal planes.

Supplementary Files

This is a list of supplementary files associated with this preprint. Click to download.

- SupplementalMaterial.docx
- Suppl5ExampleHealthyVolunteerswholeLiver.mp4
- Suppl6ExamplePediatricTomographwholeBody.mp4